ELSEVIER

Catalysis Today 63 (2000) 327–335

CATALYSIS TODAY

www.elsevier.com/locate/cattod

The reactions of ethanol over M/CeO_2 catalysts Evidence of carbon–carbon bond dissociation at low temperatures over Rh/CeO_2

A. Yee, S.J. Morrison, H. Idriss*

Materials Chemistry, Department of Chemistry, The University of Auckland, Private Bag 92019, Auckland, New Zealand

Abstract

The reactions of ethanol over Rh/CeO_2 have been investigated using the techniques of temperature programmed desorption (TPD) and FT-IR spectroscopy, in addition to steady state catalytic tests. A comparison with previous studies of ethanol adsorption over Pd/CeO_2 [J. Catal. 186 (1999) 279] and Pt/CeO_2 [J. Catal. 191 (2000) 30] catalysts is presented. The apparent activation energy for the reaction was 49, 40, and 43 kJ mol^{-1} for Rh/CeO_2, Pd/CeO_2 and Pt/CeO_2, respectively, while the turnover number (TON) at 400 K was 5.9, 8.6 and 2.6, respectively. Surface compositions of catalysts were characterised by XPS. A decrease of the atomic O(1s)/Ce(3d) ratio of the CeO_2 support indicates its partial reduction upon addition of the noble metal. The extent of reduction per metal atom was in the following order: Pt > Pd > Rh. FT-IR and TPD studies have shown that dehydrogenation of ethanol to acetaldehyde occurred over Pd/CeO_2, Pt/CeO_2 and Rh/CeO_2. Moreover, Rh/CeO_2 readily dissociated the C–C bond of ethanol at room temperature to form adsorbed CO (IR bands at 1904–2091 cm^{-1}). This was corroborated by the low desorption temperature of CH_4 over Rh/CeO_2 (450 K) when compared to that of Pd/CeO_2 (550 K) or Pt/CeO_2 (585 K).

Keywords: Ethanol dehydrogenation; TPD-ethanol; Rh/CeO_2-ethanol; Ethanol-IR; C–C bond

1. Introduction

In the last three decades, three-way catalysts (TWC) have been successfully employed in the treatment of toxic automobile exhaust emissions. The composition of these catalysts typically comprise of an active phase of noble metal (Pd, Pt and/or Rh) dispersed over an alumina support containing a number of additional components, including ceria (CeO_2). Apart from its role as an oxygen storage component [3,4], CeO_2 has also been associated with the thermal stabilisation of the alumina support [5], promotion of water-gas shift activity [6] and dispersion of the active noble metal phase [7,8]. In reductive atmospheres, Ce^{4+} ions on a stoichiometric surface are readily reduced to Ce^{3+}. This enables the reversible addition and removal of oxygen, thus allowing CeO_2 to act as an oxygen storage material in oxidation reactions. The Ce^{4+} to Ce^{3+} reduction is accompanied by the formation of oxygen vacancies leading to the formation of a Ce_2O_3 phase at high temperatures. Surface reduction of CeO_2 has been reported to occur at 473 K under H_2, with reduction temperatures above 923 K required for bulk reduction [9].

In recent years, ever increasingly stringent vehicle emission regulations have necessitated the modification and improvement of TWCs to accommodate developments in fuel formulations and alternative-fuel

* Corresponding author. Tel.: +64-9-3737599; fax: +64-9-3737422.
E-mail address: h.idriss@auckland.ac.nz (H. Idriss).

0920-5861/00/$ – see front matter
PII: S0920-5861(00)00476-4

vehicle technology. As such, oxygenated compounds, such as alcohols and ethers, have been increasingly used as fuel additives and alternative fuels. Although alcohols are considered to be clean burning fuels, their partial oxidation to aldehydes poses a greater threat as potential carcinogens. The problem of effectively controlling the emissions caused by burning these oxygenated compounds requires a better understanding of the fundamental reaction pathways along which the desired conversions occur on current commercial catalyst systems.

The reactions of ethanol have been investigated over the surfaces of metals [10–15], oxides [16–20], and metal–oxides interface [1,2,21–23]. Over clean metals such as Ni [10], Pt [11] and Pd [12], ethanol is dissociated to ethoxides and adsorbed hydrogen. Ethoxides are subsequently dehydrogenated to acetaldehyde. Over Rh (1 1 1), the reaction sequence appears different. Ethanol first dissociates to ethoxides (as in the case of Pd, Pt, or Ni) but ethoxides do not give acetaldehyde they dehydrogenate to give an oxametallacycle ((a)–OCH_2CH_2–(a)) intermediate, where (a) for adsorbed [13]. This latter decomposes to CO upon further annealing. Ethanol may also react via a carbon–carbon bond dissociation pathway on the surface of some metals. For example, ethanol gives methane over Pt (1 1 1) at 310 K [15] and over (2×1) Pt (1 1 0) at 240 K [14]. A review of the reaction mechanism of ethanol over metal single crystals can be found in [15]. Over oxides, both dehydrogenation to acetaldehyde and dehydration to ethylene occur depending on the nature of the oxide [16]. The reasons for this are numerous. Basic site density [17], bond energy [18], electronegativity difference [18], change in the Madelung potential [19], and the oxygen electronic polarisability of the oxides [20] have been proposed to influence the reaction selectivity. In general, a high basic site number, a small metal cation–oxygen anion bond energy, a small Madelung potential of O anion, and a high oxygen electronic polarisability will favour dehydrogenation rather than dehydration. CeO_2 in that regard fits this requirement.

Other secondary products mostly resulting from acetaldehyde, were also observed for the reaction of ethanol over oxides. These include: crotonaldehyde (formed by β-aldolisation of acetaldehyde) [24], ethyl acetate (formed by dimerisation of two acetaldehyde molecules), acetates (formed by direct oxidation of acetaldehyde) [17], and butenes (formed by reductive coupling of two molecules of acetaldehyde over defected sites) [25].

In an effort to elucidate the reaction pathways and mechanisms involved in the reaction of ethanol over M/CeO_2 catalysts, where M = Pd, Pt or Rh, a series of investigations were performed using temperature programmed desorption (TPD) and FT-IR spectroscopy. The adsorption, and subsequent reaction, of ethanol over the surfaces of Pd/CeO_2 and Pt/CeO_2, along with bare CeO_2, have been discussed in greater detail elsewhere [1,2]. In this work, results from the adsorption and reaction of ethanol over Rh/CeO_2 are presented and discussed with comparison to those obtained previously over Pd/CeO_2 [1] and Pt/CeO_2 [2] catalysts.

2. Experimental

2.1. Catalyst preparation and characterisation

CeO_2 was prepared by precipitating a solution of cerium(III) nitrate at pH 9 with ammonia; the resulting precipitate was filtered, dried at 373 K and calcined at 723 K for 5 h. The Pd/CeO_2, Pt/CeO_2 and Rh/CeO_2 catalysts were prepared, with 1 wt.% metal loadings, by impregnating the CeO_2 support with solutions of the appropriate chloride precursor dissolved in 1 M HCl. Specific surface area measurements were determined by the multi-point BET method [26]. Surface compositions were analysed by X-ray photoelectron spectroscopy (XPS); experimental details have been described in a previous work [1].

2.2. Steady state reactions

Kinetic analysis was conducted with a fixed-bed reactor fitted in a programmable oven with an operating range of up to 673 K and linked to a gas chromatograph (GC) via a six-way valve (containing a 1 ml loop). Ethanol, in a saturator at 273 K (vapour pressure 1.5×10^3 Pa), is sent in a dry air carrier gas giving the following molar ratio: 1.5:21:77.5 for ethanol, oxygen and N_2, respectively. Total pressure in the reactor was maintained at 1 atm. The mass of catalysts in milligram, were 98, 100, and 101 for Rh/CeO_2,

Pd/CeO_2 and Pt/CeO_2, respectively. Total flow rate = 60 ml/min. Product analyses were conducted by a GC equipped with a flame ionisation detector (FID). The GC is coupled to a PC running PEAKSIMPLE III software for data acquisition. A Chromosorb 102 column ($l = 2$ m, $d = 0.318$ cm), with nitrogen as the carrier gas, was used for separation of organic compounds at 373 K. The main reaction product is acetaldehyde at relatively low temperatures (up to about 523 K, depending on the catalyst) with traces of methane and ethane. Up to these temperatures there is a perfect mass balance between ethanol inlet and acetaldehyde + ethanol outlet. No CO nor CO_2 were observed in this temperature domain (at higher temperatures, above 600 K considerable amounts of CO and CO_2 were formed; their concentration depended on the oxygen to ethanol ratio; this point is beyond the scope of this work and is currently under investigation). The rate

$$r = \frac{\{[\text{ethanol}]\text{out} - [\text{ethanol}]\text{in}\}}{\tau} = -\frac{[\text{acetaldehyde}]\text{out}}{\tau}$$

in the 373–523 K temperature domain, where τ is the contact time, was calculated in a differential mode (conversion <10%). Errors involved in GC analysis were in the order of 3–5%. The gas, containing ethanol, was allowed to flow over the catalyst for 10 min at room temperature before samples were injected in the GC via the six-way valve. The turnover numbers are reported per surface and near surface metal as determined from XPS analyses.

2.3. Temperature programmed desorption

A detailed account of the experimental procedures and equipment used in the TPD studies can be found in a previous work [1]. Relative yields of all desorption products were determined following the work of Ko et al. [27] and other workers [24].

2.4. Infrared spectroscopy

IR spectra were recorded using a Digilab FTS-60 Fourier transform spectrometer at a resolution of 4 cm^{-1} and 100 scans per spectrum. Experimental details [1,2], including cell design [28], have been reported previously. To obtain a relatively clean surface, catalyst samples were pretreated under oxygen (1.50 Torr) at 755 K for 1 h, with fresh oxygen introduced after 30 min. Ethanol (1.50 Torr), degassed by several freeze-pump-thaw cycles, was dosed at room temperature for 3 min. The ethanol-dosed samples were sequentially heated from 373 to 673 K, with spectra recorded at 50 K increments. All spectra were collected at room temperature. The spectra presented in this work are obtained by subtraction of the spectrum of the catalyst sample prior to adsorption from that of the adsorbed sample.

3. Results

3.1. Characterisation and steady state kinetics

Table 1 presents relevant data obtained from XPS and steady state analysis. The three M/CeO_2 catalysts contained similar amounts of metal cations and were

Table 1
Summary of data obtained from XPS, BET surface area determination and steady state reactions (M: Pd, Pt, or Rh)

Catalyst	CeO_2 [1]	Rh/CeO_2	Pd/CeO_2 [1]	Pt/CeO_2 [2]
Surface area ($m^2\,g^{-1}$)	57	49	55	63
XPS M($3d_{5/2}$, $4f_{7/2}$)	–	309.5 (RhO_2) [24]	336.5 (PdO) [25]	74.0 (PtO) [26]
XPS O(1s)/Ce(3d)	2.44	1.91	1.76	1.59
XPS ΔO/at.% M[a]	–	0.53	0.96	1.58
XPS at.%	–	0.17	0.25	0.26
E_a ($kJ\,mol^{-1}$)	75	49	40	43
A ($ml\,g^{-1}\,s^{-1}$)	3.8×10^9	2.6×10^6	4.7×10^5	5.6×10^5
TON[b] at 400 K	–	5.9	8.6	2.6

[a] Is a measure of the degree of reduction of CeO_2 normalised per M. $\Delta O = 2 - x$, where x = O(1s)/Ce(3d). The value of 2 is preferred because of stoichiometry.

[b] Number of ethanol molecules converted per surface metal atom (Pd, Pt or Rh) per second.

of comparable surface areas. The unreduced catalysts contained Rh, Pd, and Pt cations, as RhO_2, PdO, and PtO, respectively. It appears that addition of these metals to CeO_2 resulted in a partial reduction of surface CeO_2. This is consistent with findings by other workers [29]. The effect of each metal on reduction of the support was however different. Rh exhibited a minimal reduction effect while Pt was the most active. The effect is even clearer if normalised per metal cation (see ΔO/at.% M, as defined in Table 1).

Steady state reactions of ethanol were conducted on all catalysts in order to calculate the apparent activation energy and turnover number (TON) values. Pd/CeO_2 was the most active catalyst followed by Rh/CeO_2 (see TON in Table 1). The reaction was first order with respect to ethanol at the conditions described in the experimental section. All M/CeO_2 catalysts exhibited lower activation energies, E_a, than bare CeO_2. The addition of the noble metal to CeO_2 reduced the activation energy of the catalyst by up to 35 kJ mol^{-1}. Although the pre-exponential factors, A, decreased upon the addition of metals to CeO_2, the decrease of E_a was large enough to enhance the overall reaction rate when compared to CeO_2 alone.

3.2. Adsorption of ethanol on Rh/CeO_2

3.2.1. Temperature programmed desorption

Temperature programmed desorption profiles of ethanol over unreduced and H_2-reduced Pd/CeO_2 and Pt/CeO_2 catalysts have been previously published [1,2]. Both catalysts were active towards ethanol dehydrogenation to acetaldehyde, the latter desorbed at ca. 400 K over Pd/CeO_2 and at 475 K over Pt/CeO_2. Evidence of benzene was clearly observed by the desorption of the characteristic *m/e* 77 and 78 at 580 K over Pd/CeO_2 and at 610 K over Pt/CeO_2. Total decomposition also occurred, evidenced by the formation of CO, CO_2 and CH_4 at ca. 600 K over both catalysts.

Fig. 1 presents ethanol-TPD over unreduced Rh/CeO_2. Three different temperature domains of desorption were observed. Unreacted ethanol was desorbed at a peak temperature of 465 K and accounted for 49% of the total products desorbed. Acetaldehyde was desorbed at the lowest temperature domain of 450 K, with a yield of 21%. Similar to the TPD of ethanol from Pd/CeO_2 [1] and Pt/CeO_2

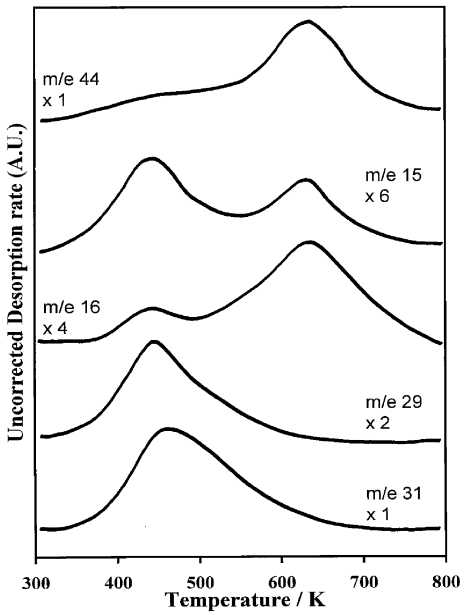

Fig. 1. Product desorption profiles from TPD after ethanol adsorption on unreduced 1 wt.% Rh/CeO_2 at 300 K.

[2], the highest temperature domain was dominated by desorptions of CO_2, CO and CH_4. Two main differences were noticed however, over Rh/CeO_2: (1) no evidence of benzene formation was observed; (2) an important desorption of CH_4 at 450 K was clearly seen. The latter point indicates that Rh/CeO_2 is more active towards carbon–carbon bond dissociation than Pd/CeO_2 or Pt/CeO_2. This observation is consistent with the ability of this catalyst to dissociate the C–C bond to form adsorbed CO as shown in IR studies (see below). Table 2 presents the carbon yield during ethanol-TPD. Unreacted ethanol contributed by up to 50% of the total desorption. Acetaldehyde was however the major reaction product (41%) followed by CO_2 (32%) while methane represented 9.5%.

Table 2
Products desorption during ethanol-TPD over 1 wt.% Rh/CeO_2

Reactant/products	Peak temperature (K)	Carbon yield	Carbon selectivity (%)
Acetaldehyde	450	0.21	41
CO_2	650	0.16	32
CO	650	0.09	18
Ethanol	465	0.49	–
CH_4	450, 650	0.02, 0.03	4.5, 5

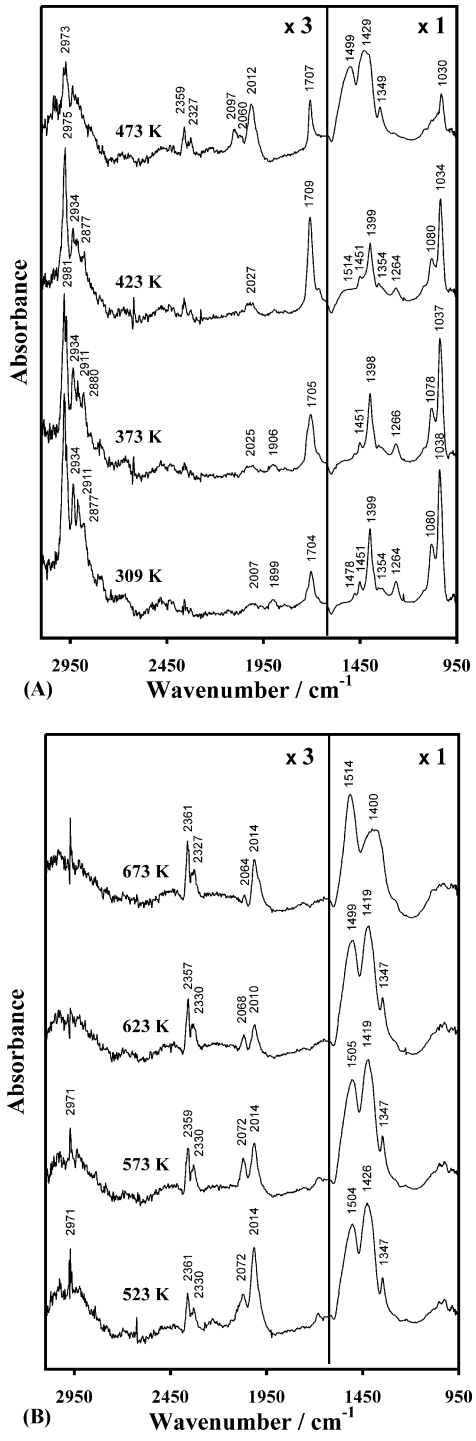

Fig. 2. FT-IR spectra after adsorption of ethanol at 309 K on unreduced 1 wt.% Rh/CeO_2 and subsequent heating to 373, 423, 473, 523, 573, 623 and 673 K.

3.2.2. Infrared spectroscopy

Fig. 2A and B present the IR spectra obtained from the adsorption of ethanol over Rh/CeO_2, at room temperature, and heated to various temperatures. The adsorption of ethanol on Rh/CeO_2 at room temperature occurred dissociatively to produce adsorbed ethoxides species; an assignment of these bands is presented in Table 3. In addition, bands attributed to η^1-adsorbed acetaldehyde, ν(C=O) at 1704 cm^{-1}, linear CO at 2007 and bridged CO at 1899 cm^{-1} were also observed. Upon heating, a general decrease in the intensity of the ethoxide bands was observed. Concomitantly, an increase in the intensity of the ν(CO) band of acetaldehyde was noticed, reaching a maximum intensity at 423 K and declining thereafter. At 473 K the decline of the band attributed to acetaldehyde coincided with the development of bands at 2097, 2060 and 2012 cm^{-1}. An increase in temperature to 523 K resulted in a clear two CO bands 2072 and 2014 cm^{-1}. IR bands attributed to Rh-gem dicarbonyl species were previously observed by several workers at 2100–2070 and 2030–2010 cm^{-1} [23,30–32]. The large difference in their relative intensity may indicate the presence of an additional linear CO at ca. 2010 cm^{-1}. The formation of carbonate species was detected at 423 K by a weak band at ca. 1500 cm^{-1}. At 473 K, this band had increased considerably together with the development of two further bands at 1429 and 1349 cm^{-1}. The intensity of these three bands increased at elevated temperatures. Like the case of Pd/CeO_2 and Pt/CeO_2,

Table 3
Assignments for ethoxide species on CeO_2 and M/CeO_2 (M: Pd, Pt, Rh) from ethanol adsorption at 309 K

Assignment	Frequency (cm^{-1})			
	CeO_2 [1]	Pd/CeO_2 [1]	Pt/CeO_2 [2]	Rh/CeO_2
ν(C–O)-*b*[a]	1057	1037	1037	1038
ν(C–O)-*m*[b]	1107	1078	1081	1080
$\delta_s(CH_3)$	1383	1397	1399	1399
$\delta_{as}(CH_3)$	nr[c]	1451	1451	1450
$\delta(CH_2)$	1473	1477	1480	1478
$\nu_s(CH_3)$	nr[c]	2880	2878	2878
$\nu_s(CH_2)$	2866	2909	2912	2911
$\nu_{as}(CH_2)$	nr[c]	2934	2933	2934
$\nu_{as}(CH_3)$	2960	2982	2977	2981

[a] *m*: monodentate.
[b] *b*: bidentate.
[c] Not resolved.

but in contrast to that of CeO_2, no evidence of acetate species was observed. This provides further evidence of the partial reduction of the support; the more reduced the surface, the less likely it contains oxygen anions of sufficient mobility to oxidise acetaldehyde to acetate species at low temperatures. Bands corresponding to CO_2 were also observed. The increase in intensity of these bands as a function of reaction temperature may indicate that it is resulting from an adsorbed CO_2 species rather than from the background (all spectra were collected at ca. 10^{-5} Torr).

4. Discussion

4.1. Ethoxide formation

FT-IR studies have shown that, over all the M/CeO_2 surfaces investigated, ethanol adsorbs dissociatively via scission of the O–H bond, as ethoxide species. An assignment of these bands is provided in Table 3. On CeO_2, the ν(C–O) bands are situated at 1057 and 1107 cm^{-1} and in the presence of the noble metal are shifted to ca. 1037 and 1080 cm^{-1}. A more elaborate discussion of the assignment of these bands is given in [2]. The presence of two distinct ν(C–O) bands indicates that two kinds of adsorbed ethoxide species are formed on the catalyst surface. The higher wavenumber band is ascribed to a monodentate ethoxide species while the lower wavenumber band to a bidentate species. Multiple adsorbed alkoxide species have been observed previously on CeO_2; Li et al. [33] identified two types of methoxide species upon adsorption of methanol on CeO_2 at 300 K, while three types of methoxides have also been reported [34,35].

The presence of metals has resulted in decreasing the IR frequency of the ν(C–O) for both the monodentate and bidentate adsorbed ethoxide species. This decrease may indicate a stronger interaction with the surface. Conversely, an increase in the IR frequencies of the $\delta(CH_3)$ and $\nu(CH_3)$ of adsorbed ethoxide species was evidenced in the presence of the metals. Invariably, a change in the electronic distribution of a bond in an adsorbate molecule will affect its force constant and consequently its vibrational frequency [36]. In this case, electrons from the O atom of the ethoxide species contribute in bonding with the surface. Subsequent redistribution of electronic charge from the CH_3– group to the O end of the molecule may effect a weakening of the bonds in the CH_3– group, hence, increasing the corresponding vibrational frequency.

4.2. Acetaldehyde and crotonaldehyde formation

The differences in acetaldehyde desorption temperature during TPD over the three catalysts may be explained as follows. Upon dehydrogenation of ethanol, acetaldehyde molecules instantaneously desorb because the energy required to dehydrogenate ethanol is higher than the desorption-energy of acetaldehyde over CeO_2 or M/CeO_2 [37]. Fig. 3 presents the desorption temperatures during TPD, as well as the TON at 400 K for these catalysts. Acetaldehyde desorbs at the lowest temperature on the most active catalyst, Pd/CeO_2, Rh/CeO_2 was next, followed by Pt/CeO_2. The order is, thus in good agreement with the steady state reaction results.

FT-IR studies have shown that at elevated temperatures ethanol-adsorbed Rh/CeO_2 catalyst experienced a general decrease in the intensity of the bands attributed to ethoxides with a concomitant appearance of bands corresponding to the formation of different reaction and decomposition products (Fig. 2). The degree of reaction and decomposition of ethanol differed greatly between this catalyst and the Pd/CeO_2 [1] and Pt/CeO_2 [2] catalysts. This is illustrated in Fig. 4 that compares the IR spectra, obtained from the adsorption of ethanol, over the surfaces of CeO_2 and M/CeO_2

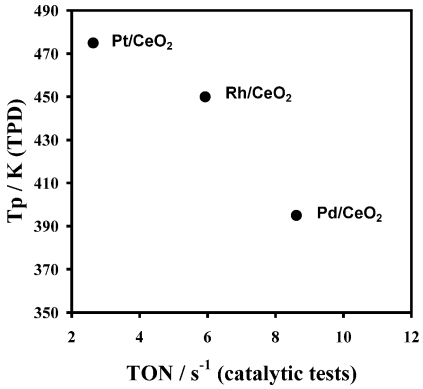

Fig. 3. Turnover numbers (TON, at 400 K), from steady state catalytic tests, of Rh/CeO_2, Pd/CeO_2 [1] and Pt/CeO_2 [2] plotted against peak desorption temperatures of acetaldehyde (*m*/*e* 29) from TPD experiments.

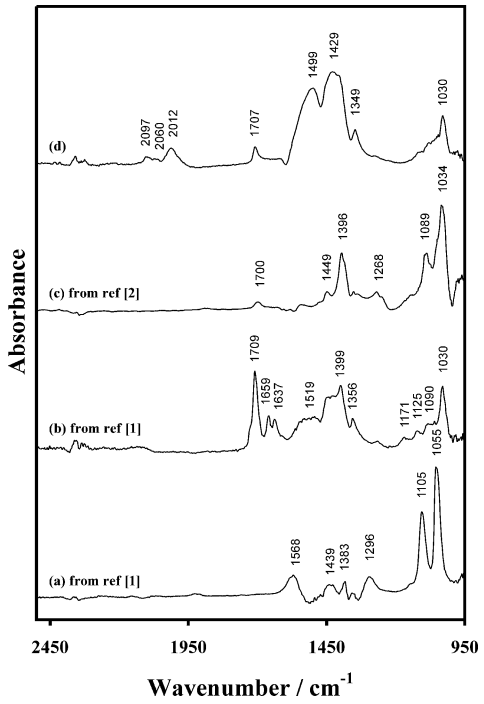

Fig. 4. FT-IR spectra after adsorption of ethanol at 309 K on unreduced CeO_2 [1], Pd/CeO_2 [1], Pt/CeO_2 [2] and Rh/CeO_2 and heated to 473 K. Spectra collected at room temperature.

at room temperature, and heated to 473 K. Adsorbed η^1-acetaldehyde, from dehydrogenation of ethoxides (Eqs. (1) and (2)), was detected on all M/CeO_2 surfaces by its ν(C=O) mode at 1700–1709 cm^{-1}.

$$CH_3CH_2OH_{(g)} + O(l) \rightarrow CH_3CH_2O_{(ads)} + OH_{(ads)}, \quad (l) = \text{lattice} \tag{1}$$

$$CH_3CH_2O_{(ads)} \rightarrow CH_3CHO_{(ads)} + H_{(ads)} \tag{2}$$

The formation of acetaldehyde is greatest in the presence of Pd (Fig. 4(b)) and smallest over Pt/CeO_2. This is in complete agreement with TPD and steady state reaction data (Fig. 3). The pair of bands at 1659 and 1637 cm^{-1} have been previously ascribed, respectively, to the ν(C=O) and ν(C=C) modes of adsorbed crotonaldehyde [1,2]. The formation of crotonaldehyde results from the β-aldolisation of acetaldehyde on the surface of CeO_2. The aldolisation reaction requires base sites to abstract an α-hydrogen atom and Lewis acid sites to bind the two molecules of acetaldehyde. Crotonaldehyde has also been observed, upon acetaldehyde adsorption, over other oxide surfaces, such as TiO_2 [24], Al_2O_3 [38] and UO_3 [39] the reaction mechanism has been presented and discussed previously [24].

4.3. C–C bond dissociation over Rh/CeO_2

The prominent feature of the reaction of ethanol over Rh/CeO_2 is its ability to readily dissociate the C–C bond of ethanol to produce adsorbed CO (Fig. 2). This attribute is evidenced by the absence of crotonaldehyde and benzene formation over this catalyst. TPD studies showed that appreciable amounts of benzene were desorbed from the surfaces of Pd/CeO_2 and Pt/CeO_2 at 580 and 610 K, respectively, as shown in Fig. 5. The absence of benzene desorption from Rh/CeO_2 is another consequence of its ability to dissociate the C–C bond.

One may view the C–C bond dissociation reaction of ethanol as a CH_3– transfer to the surface in an initial step (Eq. (3)) while the non-C–C bond dissociation

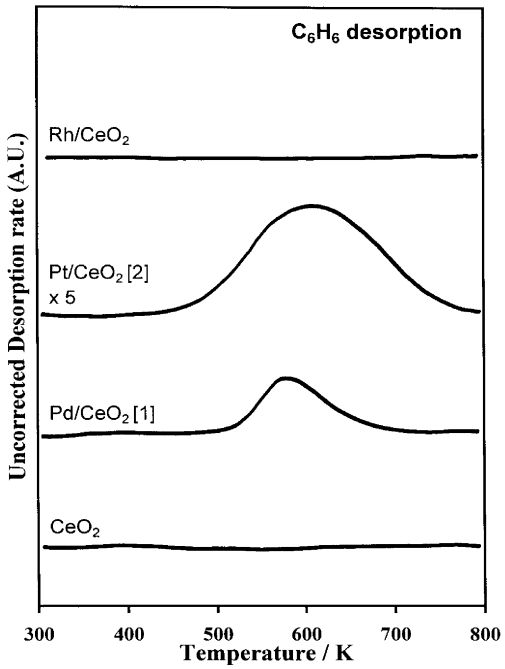

Fig. 5. Desorption profiles of benzene from the TPD of ethanol-adsorbed CeO_2, Pd/CeO_2 [1], Pt/CeO_2 [2] and Rh/CeO_2.

reactions (dehydrogenation) as a H– transfer (Eq. (2)).

$$CH_3CH_2O_{(ads)} \rightarrow CH_{3(ads)} + CH_2O_{(ads)} \quad (3)$$

Both the formation of methane in TPD and of CO in IR experiments over Rh/CeO_2 indicated that Eq. (3) proceeded further to

$$CH_2O_{(ads)} \rightarrow CO + 2H_{(ads)} \quad (4)$$

$$CH_{3(ads)} + H_{(ads)} \rightarrow CH_4 \quad (5)$$

The intrinsic barriers to the transfer of a molecular ligand (CH_3–) are much higher than those of the transfer of an atom (H–) [40]. It is thus likely that the intrinsic barrier for the methyl ligand is lower for Rh than for Pt or Pd (in the gas phase, the intrinsic barrier for CH_3– is between 80 and 90 kcal mol^{-1} [41] while it has been calculated equal to 30 kcal mol^{-1} on a Ni surface [42]). In order for a bond scission to occur, electrons are required to flow into antibonding orbitals of the adsorbate. In other words, the *d* electrons of Rh might be shared to a larger extent with the antibonding orbitals of ethoxides than those of Pd and Pt.

4.4. Effect of the nature of the metal on the reduction of CeO_2

XPS of the O(1s) and Ce(3d) regions have shown a change of the oxygen anions to cerium cations ratio, see Table 1. A plot of this change as a function of CO_2 to CO desorption during ethanol-TPD on the different catalysts ([1,2]; Tables 1 and 2) is shown in Fig. 6. The more reduced is the surface the less CO_2 will be formed. Indeed, Fig. 6 shows this trend, with Pt the most active for the partial reduction of CeO_2 (less amount of CO_2 desorbing during TPD and high values of Δx) while Rh is the least. From Fig. 6 the following empirical relationship, between the extent of reduction (as determined by XPS) and the ratio CO_2/CO (as determined by TPD), for the three metals, is obtained

$$\frac{CO_2}{CO} = 1.27\left\{\frac{[O(1s)/Ce(3d)] - 2}{[M]}\right\} + 2.43$$

where [M] is in at.% and O(1s) and Ce(3d) are the integrated and corrected XPS peak areas.

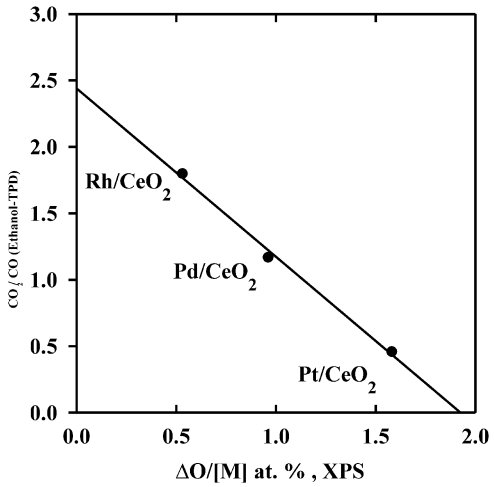

Fig. 6. CO_2/CO desorption during ethanol-TPD over Pd/CeO_2, Pt/CeO_2 and Rh/CeO_2 as a function of ΔO/at.% M (as defined in Table 1).

5. Conclusions

It has been shown that the adsorption and subsequent reaction of ethanol over Pd/CeO_2, Pt/CeO_2 and Rh/CeO_2 occurs through an ethoxide intermediate followed predominantly by an oxidative dehydrogenation reaction to yield acetaldehyde. Both the Pd/CeO_2 and Pt/CeO_2 catalysts have exhibited the ability to initiate C–C bond formation, evidenced by the production of crotonaldehyde and benzene. Unlike Pd/CeO_2 and Pt/CeO_2, Rh/CeO_2 readily dissociates the C–C bond of ethanol to produce adsorbed CO and CH_4. The absence of benzene on Rh/CeO_2 is consistent with its capacity to dissociate the C–C bond of ethanol. This work indicates that Rh lowers the intrinsic activation barrier for C–C bond dissociation more than Pd or Pt. A relationship between the extent of reduction of the noble metal, as determined from the XPS O(1s) to Ce(3d) lines, and the CO_2 to CO desorption peaks during ethanol-TPD is observed.

References

[1] A. Yee, S.J. Morrison, H. Idriss, J. Catal. 186 (1999) 279.
[2] A. Yee, S.J. Morrison, H. Idriss, J. Catal. 191 (2000) 30.
[3] H.S. Gandhi, A.G. Piken, M. Shelef, R.G. Delosh, SAE Paper 760201 (1976).

[4] E.C. Su, C.N. Montreuil, W.G. Rothchild, Appl. Catal. 17 (1985) 75.
[5] B. Harrison, A.F. Diwell, C. Hallet, Platinum Met. Rev. 32 (1988) 73.
[6] G. Kim, Ind. Eng. Chem. Prod. Res. Dev. 21 (1982) 267.
[7] S.G. Hinden, Engelhard Mineral and Chemical Co., US Patent 3,870,455 (1973).
[8] F.J. Sergeys, J.M. Masellei, M.V. Ernest, W.R. Grace Co., US Patent 3,903,020 (1974).
[9] H.C. Yao, Y.F. Yao, J. Catal. 86 (1984) 254.
[10] S.M. Gates, J.N. Russell Jr., J.T. Yates Jr., Surf. Sci. 171 (1986) 111.
[11] B.A. Sexton, K.D. Rendulic, A.Z. Hughes, Surf. Sci. 1212 (1982) 181.
[12] J.L. Davis, M.A. Barteau, Surf. Sci. 187 (1987) 388.
[13] C.J. Houtman, M. A Barteau, J. Catal. 130 (1991) 528.
[14] Y. Cong, R.I. Masel, Surf. Sci. 396 (1998) 1.
[15] Y. Cong, V. van Spaendonk, R.I. Masel, Surf. Sci. 385 (1997) 246.
[16] H. Idriss, M.A. Barteau, Adv. Catal. 45 (2000) 261.
[17] H. Idriss, E.G. Seebauer, J. Mol. Catal. A 152 (2000) 201.
[18] O.V. Kyrlov, Catalysis by Nonmetals, Academic Press, New York, 1970.
[19] S.V. Chong, T.R. Griffiths, H. Idriss, Surf. Sci. 444 (2000) 187.
[20] H. Idriss, E.G. Seebauer, Catal. Lett. 66 (2000) 139.
[21] P.O. Larsson, A. Anderson, J. Catal. 179 (1998) 72.
[22] M.J.L. Gines, E. Iglesia, J. Catal. 176 (1998) 155.
[23] J.C. Lavalley, J. Saussey, J. Lamotte, R. Breault, J.P. Hindermann, A. Kiennemann, J. Phys. Chem. 94 (1990) 5941.
[24] H. Idriss, K.S. Kim, M.A. Barteau, J. Catal. 139 (1993) 119.
[25] H. Idriss, M.A. Barteau, Catal. Lett. 40 (1996) 147.
[26] S. Brunauer, P. Emmett, E. Teller, J. Am. Chem. Soc. 60 (1938) 309.
[27] E.I. Ko, J.B. Benziger, R.J. Madix, J. Catal. 62 (1980) 264.
[28] G.J. Millar, D. Newton, G.A. Bowmaker, R.P. Cooney, Appl. Spectrosc. 48 (1994) 827.
[29] A. Trovarelli, Catal. Rev. 38 (1996) 439 and references therein.
[30] J.A. Anderson, C.H. Rochester, Z Wang, J. Mol. Catal. A 139 (1999) 285.
[31] D.A. Bulushev, G.F. Froment, J. Mol. Catal. A 139 (1999) 63.
[32] J.T. Yates Jr., T.M. Duncan, S.D. Worley, R.W. Vaughan, J. Chem. Phys. 70 (1979) 1219.
[33] C. Li, K. Domen, K. Maruya, T. Onishi, J. Catal. 125 (1990) 445.
[34] J. Lamotte, V. Moravek, M. Bensitel, J.C. Lavalley, React. Kinet. Catal. Lett. 36 (1988) 113.
[35] C. Binet, A. Badri, J.C. Lavalley, J. Phys. Chem. 98 (1994) 6392.
[36] C.N.R. Rao, Chemical Applications of Infrared Spectroscopy, Academic Press, New York, 1963.
[37] H. Idriss, C. Diagne, J.P. Hindermann, A. Kiennemann, M.A. Barteau, J. Catal. 155 (1995) 219.
[38] H. Madhavaram, H. Idriss, in preparation.
[39] H. Madhavaram, H. Idriss, Catal. Today, in press.
[40] R.I. Masel, Principles of Adsorption and Reaction on Solid Surfaces, Wiley, New York, 1996.
[41] F. Westley, Table of Recommended Rate Constants for Chemical Reactions Occuring in Combustions, NBS, Washington, DC, 1980.
[42] J.A. Dumesic, The Microkinetics of Heterogeneous Catalysis, American Chemical Society, Washington, DC, 1993.